.

Citation: *Egypt.Acad.J.Biolog.Sci. (C.Physiology and Molecular biology) Vol. 16(1) pp23-46 (2024)*
DOI: 10.21608/EAJBSC.2024.335612

Egypt. Acad. J. Biolog. Sci., 16(1):23-46 (2024)

Egyptian Academic Journal of Biological Sciences
C. Physiology & Molecular Biology
ISSN 2090-0767
www.eajbsc.journals.ekb.eg

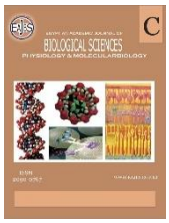

The Implication of Altered DKK1/LRP/β-catenin Signaling in Dexamethasone Induced Bone Remodeling Disruption: *In Silico* and *In Vivo* Studies in Male Rats

Adham M. Maher[1*], Samar R. Saleh[1], Doaa A. Ghareeb[1], Eman Sheta[2], Mohamed Nabil[3], Fatema A. Younis[1] and Aliaa A. Masoud[1]

[1]Department of Biochemistry, Faculty of Science, Alexandria University, Alexandria, 21511, Egypt.
[2]Department of Pathology, Faculty of Medicine, Alexandria University.
[3]Pharmacology Department, Faculty of Pharmacy, New Valley University, Kharga 72511, Egypt.

***E-mail:** adham.mostafa@alexu.edu.eg

ARTICLE INFO

Article History
Received:5/12/2023
Accepted:10/1/2024
Available:14/1/2024

Keywords:
Glucocorticoids, HSCs, MSCs, Oxidative stress, Osteoporosis, Wnt signaling.

ABSTRACT

Background: Long-term glucocorticoid administration represents the main source of 2ry osteoporosis, jeopardizing bone to fracture and loss. This study presents an innovation regarding the alterations in the osteoporotic Wnt/β-catenin signal encouraged by dexamethasone through studying some markers implicated in the proliferation and differentiation of the major bone remodeling cells using *in silico* and *in vivo* studies. **Methods and Results:** Docked models were used to visualize and evaluate the binding of dexamethasone (DEXA) towards main bone remodeling modulators. Regarding the *in vivo* study, sixteen Sprague-Dawley adult males were designated into a control group administered saline, and an osteoporosis-induced group was administered 1 mg/kg DEXA intraperitoneally daily for 6 weeks. The molecular docking demonstrated binding and interactions between DEXA and main bone remodeling targets. DEXA treatment caused osteoporotic changes in femoral microscopy, increased femoral oxidative stress, elevated proliferation markers, raised osteoblast differentiation inhibitor**,** diminished markers for osteoblasts differentiation, and increased markers for differentiation of osteoclasts and adipocytes. **Conclusions:** Glucocorticoid-induced osteoporosis is manifested through an intensified proliferation of HSCs and MSCs via escalating and changing the Wnt signaling, which acts as a communicator between both cell populations. These alterations brought about the track-change of MSCs differentiation from the osteoblastic to the adipocytic track and accelerated osteoclastic differentiation.

INTRODUCTION

Glucocorticoids (GCs) have been widely used for more than 70 years (Annane, 2021). Hench was awarded the Nobel Prize in 1950 for GCs discovery and its effects on established rheumatoid arthritis (Jung *et al.*, 2008). Since then, exogenous GCs such as dexamethasone (DEXA) and prednisolone, have been widely prescribed in treating various inflammatory, autoimmune, and allergic disorders, such as the current pandemic COVID-19, rheumatoid arthritis, transplant rejection, and asthma (Vandewalle *et al.*, 2018; Annane, 2021). However, GC administration is associated with iatrogenic complications earned to two facts; first is the fundamental role of GCs in metabolic homeostasis, inflammation, as well as cell proliferation and differentiation (Rhen and Cidlowski, 2005; Vandewalle *et al.*, 2018).

Second is that the doses required to achieve or maintain these equivalent efficacies are often higher than the actual required dose. Moreover, the long-term use of GC affects its perceived safety advantages (Chotiyarnwong and McCloskey, 2020). Some of the common iatrogenic complications associated with GC administration include centripetal obesity, insulin resistance, diabetes mellitus, immunodeficiency, infertility, and glucocorticoid-induced osteoporosis (GIO) (Buckingham, 2006).

Bone is a dynamic mineralized connective tissue under continuous remodeling through the balanced collaboration between the two main bone cell types; the bone-forming osteoblasts and the bone resorptive osteoclasts and their adult stem cells proliferating precursors (Chalmers, 1978; Marie, 1992; Frenkel *et al.*, 2015). Osteoblasts originate from mesenchymal stem cells (MSCs). These stem cells can also develop into other cell lineages as adipocytes and chondrocytes (Saud, Malla and Shrestha, 2019). In contrast, osteoclasts originate from hematopoietic stem cells (HSCs) (Martin, Sims and Quinn, 2011).

Osteoporosis (OP), a silent bone metabolic disorder, increased in prevalence while remaining largely underdiagnosed and undertreated. OP is depicted by an impaired bone microarchitecture and mass, affecting its strength and greatly increasing the risks of bone fracture, bone deformity, morbidity, and mortality (Lin and Lane, 2004; Wang *et al.*, 2020).

Long-term administration of synthetic GCs can trigger secondary osteoporotic features in males and females. These features encompass enhanced osteoclasts differentiation, inhibited osteoblastogenesis, and promoted osteoblasts apoptosis, causing an intensified bone resorption and a declined bone formation (Chiodini *et al.*, 2020; Chotiyarnwong and McCloskey, 2020). *In vivo* studies present an intricated and integrated phenotype provided by the real microenvironment of their cellular compartments (Sui *et al.*, 2018). The redundant cellular compartment of the bone marrow niche provides these cells with complex activities and a variety of signaling pathways, however, the exact role of each cell type remains a mystery and an opportunity for researchers (Takam Kamga *et al.*, 2021). Extensive *in vitro* and *in vivo* studies describe the onset of GIO. Yet, none of these studies were able to determine whether the increased adipocytes and osteoclasts were from a direct differentiation from an existing pool of their precursors or an increase in the proliferation of these precursors. Former *in vitro* studies described the capability of GCs to boost the proliferation of HSCs and MSCs through the activation of the Wnt/β-catenin signal in these cells, though this hasn't been reported *in vivo* studies (Han *et al.*, 2019). Molecular docking analysis is a discipline of bioinformatics and a computational biological tool used to predict, determine, and evaluate the effects of specific compounds on the action of several biological targets (García-Moreno *et al.*, 2023). Here, a wide array of markers involved in the proliferation and differentiation of bone remodeling cells were collectively measured in bone tissue. With the aid of docking analysis, the *present in silico* and *in vivo* studies provide a new perspective regarding the association between GCs and altered Wnt/β-catenin signal in the bone tissue of adult male Sprague-Dawley rats.

MATERIALS AND METHODS

1-Chemicals:

Dexamethasone, p-nitrobenzyl chloride, thiobarbituric acid, 5,5′-dithio-bis-2-nitrobenzoic acid, cumene H_2O_2, and reduced glutathione (GSH) were acquired from Sigma-Aldrich (St. Louis, MO, USA). ELISA kits for peroxisome proliferator-activated receptor (PPARγ), CD90, Osteocalcin (OCN), p38, and tartrate-resistant acid phosphatase (TRAP) were bought from INOVA, China. The total protein kit and Alkaline phosphatase (ALP) kit were bought from Spectrum, Egypt. Furthermore, qPCR kits were purchased from iNtRON Biotechnology, Korea; including total RNA

extraction (Easy redTM), cDNA synthesis, and 2X SYBR green master mix. In addition, primers of the main bone remodeling targets were acquired from Invitrogen, Thermo Fisher Scientific, USA. Other high-grade chemicals were also obtained.

***2-In silico* Bioinformatics Analysis:**

Dynamic molecular docking simulation analyses was carried out to visualize, predict, and evaluate the interactions between DEXA (MF: $C_{22}H_{29}FO_5$, MW:392.5g/moL, CID:5743) and some of the bone remodeling modulators as the crystal structures of homo sapiens β-catenin (PDB DOI:7ZRB, 3.43Å) (Low *et al.*, 2021; Wang, Li and Ji, 2021; Nalli *et al.*, 2022), tartrate-resistant acid phosphatase (TRAP, PDB DOI:2BQ8, 2.20Å) (Sträter *et al.*, 2005), ligand-binding domains (LBDs) of peroxisome proliferator-activated receptor γ (PPARγ, PDB DOI:1I7I, 2.35Å) (Cronet *et al.*, 2001), Low-density-lipoprotein (LDL) receptor-related proteins 5/6 (LRP5/6)-Dickkopf 1 (DKK1) complex (LRP6-DKK1, PDB DOI:3S8V, 3.10Å) (Cheng *et al.*, 2011), and receptor activator of nuclear factor kappa B ligand-Osteoprotegerin complex (RANKL-OPG, PDB DOI:3URF, 2.70Å) (Luan *et al.*, 2012), The crystal structure protein files were obtained as a PDB format from the RCSB-PDB database (http://www.rcsb.org/). The chemical structure of DEXA was obtained from the PubChem database (https://pubchem.ncbi.nlm.nih.gov/). By the ACD/ChemSketch software, DEXA was drawn, cleaned, optimized, and observed as a .mol format file. Then, it was converted to the PDB format file by using OpenBabel v2.3.2 software. Furthermore, protein energy minimization was carried out by using the Swiss-PDBViewer v4.1.0 program. The molecular docking simulation tool; Autodock 4.2.6, was utilized to explore the ligand-protein estimated free energy binding scores (Kcal/moL). The grid box properties were 0.375Å spacing, 13.531X-, 40.148Y-, and 78.91Z-center as well as 180 as a number of points in X-, Y-, and Z-dimensions. If the binding energy is <−5 kJ/moL, it represents that the targets have a certain binding affinity toward their ligand (Gaillard, 2018). The lowest estimated binding energy represents the best docking effect. After docking, DEXA with the lowest estimated free energy of binding toward β-catenin(B), TRAP(X), PPARγ(B), LRP6(A)-DKK1(X), and RANKL(A)-OPG(Z) chains, was selected to visualize the ligand-protein interaction by using LigPlot+ v.2.2.7 software.

3-Experimental Design:

All animal procedures obeyed the ARRIVE guidelines and were executed in compliance with the Institutional Animal Care and Use Committee (IACUC Protocol Approval No: 44-13M-9021), Alexandria University. This fulfills the guides for laboratory animal care and use announced by the National Institutes of Health (NIH Publications No. 8023). The study received an ethical clearance from the research ethics review committee, at Alexandria University (04/23/04/27/634). Sixteen male adult rats (150-170 g) of the Sprague-Dawley strain were obtained from the animal house belonging to the Graduate Studies and Research Institute, Alexandria University, Alexandria, Egypt. Polypropylene cages (4 animals/cage) were used for rat housing, a normal standard diet was used for animal feed and tap water was accessible. Animals were in a controlled healthy environment with a well-aerated room and allowed a 12/12h light-dark cycle. Following one week of adaptation, rats were aimlessly partitioned into two groups (8 animals/group) as follows: the normal control group received saline (0.9% NaCl, 1 ml, i.p.) and GCs-induced osteoporosis group that administrated 1 mg/kg dexamethasone intraperitoneally daily for 6 weeks (Takahashi *et al.*, 2010).

4-Blood And Bone Tissue Sampling And Preparation:

Following the experimental period, isoflurane inhalation was used to anesthetize overnight fasting rats. Blood samples were preserved at room temperature for 15 min to permit clotting. Blood was centrifuged at 3000 rpm at 4°C for 15 min to obtain serum, then stored at -20ºC for analysis. The entire left and right femurs were instantly isolated

from all animals. Followed by rapid removal of femoral muscles and connective tissues. Four right femurs were collected for fixation in 10% neutral buffered formalin from each experimental group for histopathological examination. The values of bone mass were determined using the remaining four right femurs. Furthermore, the left femurs were washed with iced saline, crushed using liquid nitrogen, randomly allotted into 2 portions, and reserved at -80^{o}C until usage. One portion was used to estimate the values of the relative mRNA expression and protein content of the main bone target genes and proteins, respectively. The other was homogenized into 4 volumes of iced phosphate-buffered saline (0.1 M, pH 7.4). For biochemical estimation, the bone homogenates were submitted for centrifugation at 4000 rpm for 15 min at 4°C, and the supernatant was kept at -80 °C.

5-Determination of Bone Mass:

Dual-energy X-ray absorptiometry was utilized to detect femoral bone mineral content (BMC, g) and bone mineral density (BMD, g/cm^2). The detection was held in Bone Minerals Densitometry Unit, Medical Service Unit, National Research Center, Dokki, Egypt. BMD was evaluated as a BMC/bone area value.

6-Spectrophotometry Assessments:

The activity of serum alkaline phosphatase (ALP, EC 3.1.3.1., U/L) was spectrophotometrically estimated in accordance with the manufacturer's procedure provided by Spectrum Company, Egypt. The concentrations of femoral bone thiobarbituric acid reactive substances (TBARS, µmol/mg protein), nitric oxide (NO, µmol/g protein), and reduced glutathione (GSH, µmol/mg protein) were measured using previous methods (Ellman, 1959; Tappel and Zalkin, 1960; Montgomery, H.A.C. and Dymock, 1961). Furthermore, the activities of femoral bone glutathione-S-transferase (GST, EC 2.5.1.18, U/mg protein), glutathione peroxidase (GPx, EC 1.11.1.9, U/mg protein), and superoxide dismutase (SOD, EC 1.15.1.1, U/mg protein) were measured using standardized methods (Paglia and Valentine, 1967; Habig, Pabst and Jakoby, 1974; Marklund and Marklund, 1974).

7-ELISA Analysis:

The levels of OCN, PPARγ, TRAP, and p38 mitogen-activated protein kinase (p38-MAPK) were estimated in femoral bone homogenate using a sandwich ELISA kit (INOVA, China) respecting the manufacturer's instructions. The values of bone p38 MAPK, and TRAP content were calculated in ng/mg protein, while bone OCN and PPARγ were calculated in pg/mg protein. Bone content of Cluster Differentiation (CD105), Glycogen synthase kinase 3β (GSK3β), phospho-GSK3 (GSK3βpS$_9$), and β-catenin were assessed by manual quantitative ELISA technique in accordance with the kit manufacturer's directions consuming rabbit polyclonal CD105 (# PA5-80582, Invitrogen, USA), rabbit monoclonal β-catenin (#8480, Cell Signaling Technology, USA), rabbit monoclonal GSK3β (#9315, Cell Signaling Technology, USA), and rabbit polyclonal GSK3β pS$_9$ (#abx328236, abbexa, China). Briefly, in the wells of a polyvinyl chloride microtiter plate duplicate samples were prepared by the dilution of 100 µg protein using a coating buffer (bicarbonate/carbonate, 0.2M, pH 9.6) followed by overnight incubation at 4 °C. Bovine serum albumin (BSA), 5% was used as a blocking solution to block the remaining protein binding sites in the coated wells. 1% blocking solution was consumed to dilute primary and secondary antibodies to decrease non-specific binding. The substrate solution (ρ-nitrophenyl phosphate disodium salt, PNPP) was added after incubation with primary and secondary antibodies (Goat anti-rabbit IgG, ALP, #A8025, Sigma-Aldrich, USA). Sodium hydroxide (3 M) was utilized to stop the reaction. a using the plate reader (Saniafi Diagnostics Pasteur, France), the developed color was read at 450 nm. For each protein, a standard curve was illustrated. The values of bone GSK3β and GSK3βpS$_9$ were calculated in µg/mg protein, while CD105 concentration was expressed in ng/mg protein, whereas the level of femoral bone β-catenin was measured as pg/mg protein.

8-Quantitative Real-Time Reverse Transcription PCR (qRT-PCR) Analysis:

MIQE guidelines were used for qRT-PCR. In accordance with the manufacturer's protocol provided with redTM total RNA extraction kit (iNtRON Biotechnology, Korea), total RNA was isolated from the femur and measured spectrophotometrically. To obtain the reverse transcript of total RNA, Maxime RT PreMix kit (iNtRON Biotechnology, Korea) was utilized following the manufacturer's procedure. qRT-PCR assessment was executed as follows: in each well, a total volume of 20 µl was prepared by adding 1 µl of cDNA, 10 µM specific primers, 10 µl RealMOD™ Green w2 2X qPCR mix (iNtRON Biotechnology, Korea), and RNase-free water. Samples were loaded in duplicate. Sequences of the studied genes primers and the qRT-PCR conditions are described in Table 1. The amplification step for qPCR was accomplished with 35-40 cycles of 95°C for 20 sec, 43- 60°C for 30 sec and 72°C for 60 sec. Roto Gene Q 5Plex HRM (Qiagen, Hilden, Germany) with a Rotor-Gene Q software was used for the qRT-PCR analysis. The comparative $2^{-\Delta\Delta CT}$ method was used. The mRNA level of the Glyceraldehyde 3-phosphate dehydrogenase (GAPDH) gene was used to normalize all values. Using the calibrator results of sham control, results were expressed as the n-fold increase in gene expression. Following is the primer sequences of the used targeted genes: Low-density lipoprotein receptor-related protein-5 (LRP5) (Lu *et al.*, 2017), Dickkopf-related protein 1 (DKK_1) (Caricasole *et al.*, 2004), Wingless protein 5a (WNT5a) (Pizzino *et al.*, 2017), Sclerostin (SOST) (Chen *et al.*, 2016), Runt-related transcription factor 2 ($RUNX_2$) (Han *et al.*, 2015), Osterix (OSX) (Liao *et al.*, 2017), Collagen, type I, alpha 1 (COL1A1) (Chen *et al.*, 2016), Osteoprotegerin (OPG) (An *et al.*, 2007), Receptor activator of nuclear factor kappa-B ligand (RANKL) (An *et al.*, 2007), and Glyceraldehyde 3-phosphate dehydrogenase (GAPDH) (Maher *et al.*, 2020).

Table 1. Primers sequence and qRT-PCR conditions.

Gene name/ Accession Number	Primer Sequence		Annealing Temperature (°C)	Number of cycles
GAPDH/ NM_017008.4	F	5'- AGATCCACAACGGATACATT - 3'	52	35
	R	5'- TCCCTCAAGATTGTCAGCAA - 3'		
LRP5/ NM_001106321.2	F	5'-CTGCCAGGATCGCTCTGATG-3'	57	40
	R	5'- ACACTGTTGCTTGATGAGGACACAC-3'		
OPG/ NM_012870.2	F	5'- GTTCTTGCACAGCTTCACCA-3'	54	40
	R	5'- AAACAGCCCAGTGACCATTC-3'		
RANKL/ NM_057149.1	F	5'- ACCAGCATCAAAATCCCAAG-3'	52	35
	R	5'- GGCCGCTAATTTCCTCACCA-3'		
DKK1/ NM_001106350.1	F	5'- GCTGCATGAGGCACGCTAT-3'	55	35
	R	5'- AGGGCATGCATATTCCGTTT-3'		
Wnt5a/ NM_022631.3	F	5'- CCATGAAGAAGCCCATTGGAATA-3'	60	40
	R	5'- GGCCAAAGCCATTAGGAAGAA-3'		
SOST/ NM_030584.2	F	5'- GTGCAAGTGCAAGCGCCTCA -3'	60	40
	R	5'- GCTCCGCCTGGTTGGCTTTG -3'		
RUNX2/ NM_001278483.1	F	5'- AGTGTGTGTGTCCGCATGAT -3'	56	40
	R	5'- CCACTTGGGGTCTAAGAACG -3'		
OSX/ NM_181374.2	F	5'- TGAGGAAGAAGCCCATTCAC -3'	53.5	40
	R	5'- ACTTCTTCTCCCGGGTGTG -3'		
COL1A1/ NM_053304.1	F	5'- CAAGGACTATGAAGTTGATGC-3'	43	40
	R	5'- ACCAGTAGAGAAATCGCAGT-3'		

GAPDH, glyceraldehyde phosphate dehydrogenase; LRP5, low-density lipoprotein receptor-related protein 5; OPG, osteoprotegerin; RANKL, receptor activator for nuclear factor-kappa B ligand; DKK1, Dickkopf Wnt signaling pathway inhibitor 1; Wnt5a, Wnt Family Member 5a; SOST, sclerostin; SOX9, SRY-Box Transcription Factor 9; RUNX2, Runt-related transcription factor 2; OSX, osterix and COL1A1, collagen type 1 alpha 1.

9-Histopathological Study:

Fixation of right femoral bone samples was carried out using 10% neutral buffered formalin for 72 h, then embedded in 10% neutral buffered EDTA solution (pH 7.4) for one week to allow decalcification. Furthermore, the femoral bone samples were dehydrated and embedded in a paraffin using a reference standard method (Bancroft, J.D. and Gamble and Burchette, 2009) A rotary microtome (Leica RM2125 RTS, Germany) was used to cut bone samples into 5 µm sections. Then sections were examined under light microscopy (Olympus CX23

microscope) after staining with hematoxylin and eosin (H&E) to evaluate the histopathological changes. Two independent histopathological features were used to estimate the morphological results. The metaphysis was determined for assessing trabecular bone quality. In previous studies, the scoring system was clearly explained, in which score 0 represents normal structure, score 1 demonstrates a partial reduction in the trabecular bone, score 2 represents a great reduction, and score 3 shows a complete absence in the trabecular bone (Bitto *et al.*, 2009; Pizzino *et al.*, 2017). The trabecular bone area (TBA) percentage was also measured. 90–100% bone area was counted as score 0, 60–90% was considered as score 1, 30–60% was expressed as a score 2, whereas TBA <30% was given a score 3. Epiphyseal plate thickness was assessed using 40X power. Moreover, osteoblasts rimming cortical bone count was estimated using one high power field (HPF). A computerized image analysis program (Leica Application Suite 4.12.0) was used to analyze these bone features. The presence of fat cells (necrotic features) in the bone marrow was also examined.

10-Analysis of the Study's Statistics:

Data were stated as a mean ± SD. LSD *post hoc* analysis of the one-way ANOVA test (SPSS 16.0 software, Chicago, IL, USA) was exploited to statistically estimate differences within groups. Results values are considered statistically significant at $*p < 0.05$.

RESULTS

1-Visualization of the Computational Biology Docked Forms:

The lowest estimated free energy of binding scores for DEXA toward β-catenin, TRAP, PPARγ, LRP5/6-DKK1, and RANKL-OPG complexes were -8.71, -10.44, -12.92, -12.08, and -9.69 kcal/mol, respectively. Furthermore, the estimated inhibition constant (Ki) values of DEXA toward these targets were 414.69 nM, 22.25 nM, 338.99 pM, 1.41 nM, and 78.81 nM, respectively. DEXA associates with β-catenin residues through one H-bond (Tyr331B) and several electrostatic and hydrophobic interactions (Tyr331, Lys288, Leu286, Ala284, Asn287, Ser318, Gly319, Val283, Ala323, Asn326, and Ile327B), Fig. 1A. DEXA associated with residues of extracellular domains of LRP5/6 receptor through one H-bonds (Leu753A) and several electrostatic and hydrophobic interactions (Gln887, Tyr800, Trp714, Leu755, Asp668, Leu667, Met710, Leu753, Asn794, Ala752, Leu880, Thr797, Leu796, Thr839, Ala711, Phe669, and Arg886A) (Fig. 1B.) Furthermore, DEXA interacted with PPARγ residues of its LBDs through four H-bonds (Leu228, His266, and two H-bonds with Lys265B) and several electrostatic and hydrophobic interactions (Arg288, Pro227, Leu228, Glu291, His266, Phe264, Lys263, Lys265, Ser342, Ile341, Glu343, and Glu295B) (Fig. 1C). DEXA also correlates with residues of TRAP repression loop, eliminating its activity through three H-bonds (Ser97, Arg155, and Asp156A(X)) and several electrostatic and hydrophobic interactions (Ser97, Val96, His92, Asn142, Arg155, Gly141, Val137, Pro154, Asp156, Thr138, and Asn95A(X)) (Fig. 1D). Residues of C(X) chain of DKK1 correlated with residues of extracellular domains of LRP5/6(A) receptor through 7 H-bonds which are Tyr875(A)-Leu231(X), His834 (A) -Ser228(X), Asp811(A)-Arg236(X), Arg792 (A)-Phe234(X), Arg792(A)-Glu232(X), Glu 769(A)-Val219(X), and Glu708(A)-His204 (X). Moreover, several electrostatic and hydrophobic interactions (Arg792(A)-Arg236(X), Arg754(A)-Phe234(X), Pro338 (A)-Val219(X), Glu708(A)-Phe205(X), Trp 330(A)-Phe234(X), and Tyr875(A)-Ile233(X)) were also involved (Fig. 2A).

Fig. 2B showed that residues of the A chain of RANKL associated with residues of the B(Z) chain of OPG through 6 H-bonds (Arg284(A)-Glu58(Z), Lys282(A)-Glu58(Z), Lys257(A)-Glu95(Z), Tyr241(A)-Glu95(Z), Lys181(A)-Ile94(Z), and His180(A)-Glu93(Z)) and electrostatic and hydrophobic interactions (Lys248(A)-Ser56(Z), Met239 (A)-Glu95(Z), Ser294(A)-Ile94(Z), Glu237 (A)-Phe96(Z), Ser179(A)-Glu93(Z), and His180(A)-Glu116(Z)). Fig. 2C illustrated

that DEXA interacted with residues of RANKL(A)-OPGB(Z) complex, destabilized RANKL/OPG interaction and potentiated the inhibitory effect of RANKL through one H-bonds (Ser52Z) and many electrostatic and hydrophobic interactions (Tyr49, Leu60, Ser56, Glu58, His54, Thr55, Lys22, Trp53, Ser52, Asp51, Thr50Z, and Lys248A).

2-Histopathologic Changes Associated With Dexamethasone Administration:

As demonstrated in Fig. 4 (upper panel), the control rats showed normal histological features that included a normal epiphyseal plate thickness (480-557 µm), architecture of bone trabeculae with a normal bone marrow space, and high osteoblastic count on a cortical bone surface (15-22/HPF). In their lacunae, osteocytes were observed that diminished any osteoclastic features. Furthermore, the bone marrow space contained few adipocytes. The quality of bone trabeculae was thick and continuous. Their TBA was scored as 0 score. On the other hand, DEXA administration greatly developed osteoporotic features, which reduced epiphyseal plate thickness (96 µm), showed structural deterioration of thinned bone trabeculae, and demonstrated fragmented thinned bony ossicles separating with expanded bone marrow and a great increase in the fat content (Fig. 4A, lower panel). The DEXA-treated rats also demonstrated irregularities in their architecture of bone trabeculae that were scored as score 2. Moreover, DEXA administration developed 0-30% TBA as a score of 3. In addition, DEXA administration greatly decreased osteoblastic count on a cortical bone surface (4/HPF) and increased osteoclastic activity with erosion cavity (Fig. 4A, lower panel) and necrotic osteocytes.

3-BMD and BMC:

Regarding BMD and BMC, rats treated with dexamethasone showed a significant ($p < 0.05$) reduction in these measurements by comparing with the control group (Fig. 3B).

4-Dexamethasone Triggered Alterations In Proliferation Indices:

Fig. 4 illustrates the changes in proliferation markers after DEXA injections, treating male rats with DEXA developed a significant ($p < 0.05$) rise in CD90 and CD105 protein levels compared to the control group. Furthermore, a significant ($p < 0.05$) elevation in the bone protein content of β-catenin in the homogenate of DEXA-treated rats was reported compared to rats receiving saline. Also, a significant ($p < 0.05$) elevation in the bone protein contents of GSK3βpS$_9$ and GSK3β together with the GSK3βpS$_9$/GSK3β ratio was observed compared to control rats. Likewise, DEXA-treated rats showed a significant ($p < 0.05$) rise in LRP5 fold change.

5-Effect of DEXA Treatment on Osteogenic and Adipogenic Biomarkers:

Following DEXA treatment, the osteogenic and adipogenic biomarkers; Wnt5a, SOST and DKK1 showed a significant ($p < 0.05$) increase in their fold change as opposed to the control rats. These rats also presented a significant ($p < 0.05$) decrease in the fold change of RUNX2 and OSX, along with a significant ($p < 0.05$) decline in the fold change of COL1A1 contrasted to control rats. The OCN bone protein content was significantly ($p < 0.05$) diminished compared to the control group. In addition, serum ALP and PPARγ bone protein content were significantly ($p < 0.05$) increased as a result of the DEXA treatment compared to control rats (Fig. 5).

6-Dexamethasone Encouraged HSCs Differentiation Into Osteoclasts:

Contrasting with the control rats receiving saline, a significant ($p < 0.05$) declined fold change of OPG was noted in male rats receiving DEXA. Conversely, a significant ($p < 0.05$) rise in RANKL fold change was also detected in these rats, with a consequent significant ($p < 0.05$) amplification in RANKL/OPG ratio contrasted to control rats. Furthermore, DEXA triggered a significant ($p < 0.05$) elevation in the bone protein content of p38. In addition, a significant ($p < 0.05$) boost in TRAP protein content was detected in rats receiving DEXA match-up with control rats (Fig. 6).

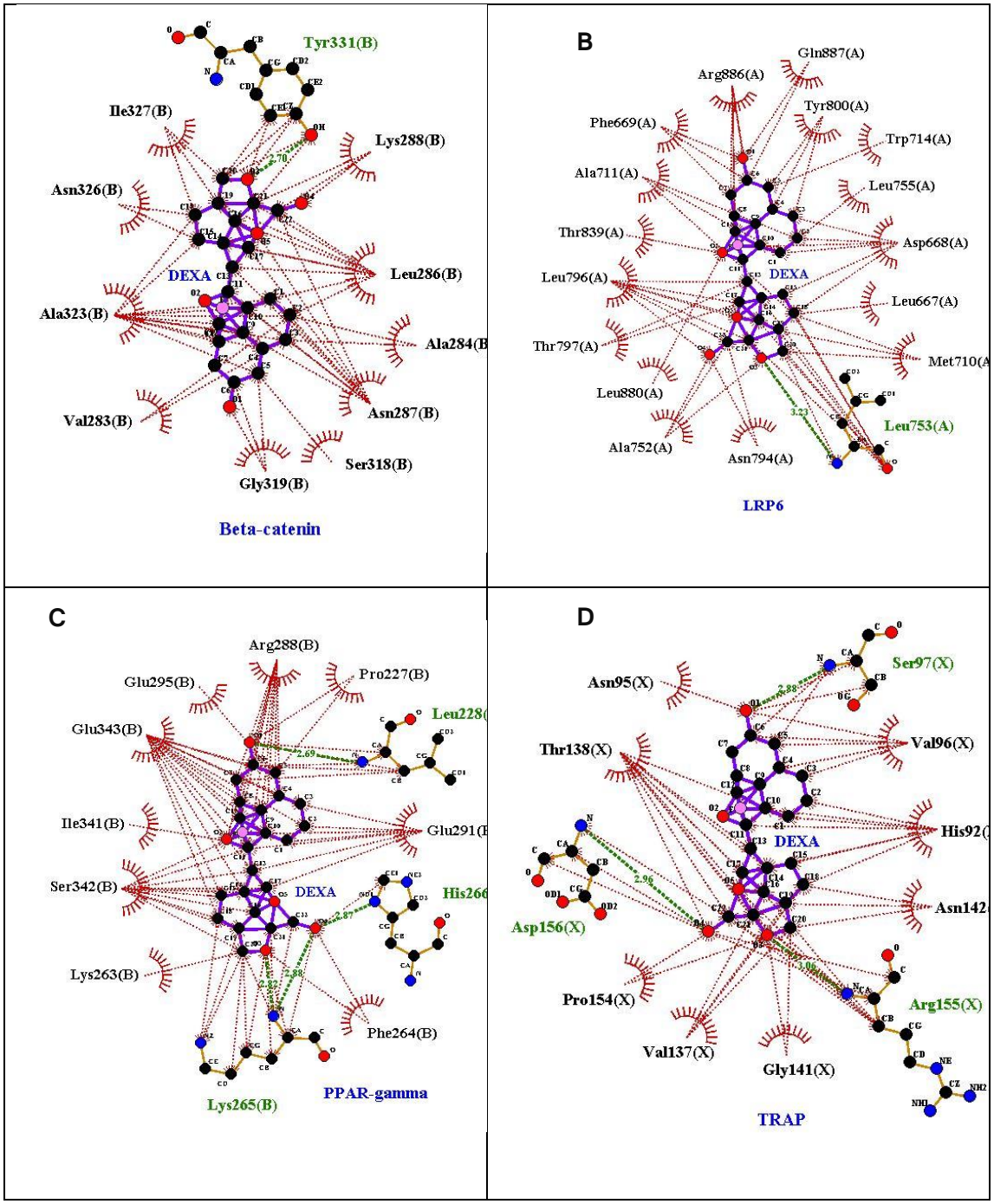

Fig. 1. 2D docked structures visualized by using LigPlot+ v.2.2.7 software. **A.** DEXA-β-catenin, **B.** DEXA- LRP5/6, **C.** DEXA-PPARγ, and **D**. DEXA-TRAP docked forms. Dotted green lines represented the ligand-amino acid residue in H-bonds, and dotted red lines demonstrated the ligand-amino acid residue in hydrophobic interactions.

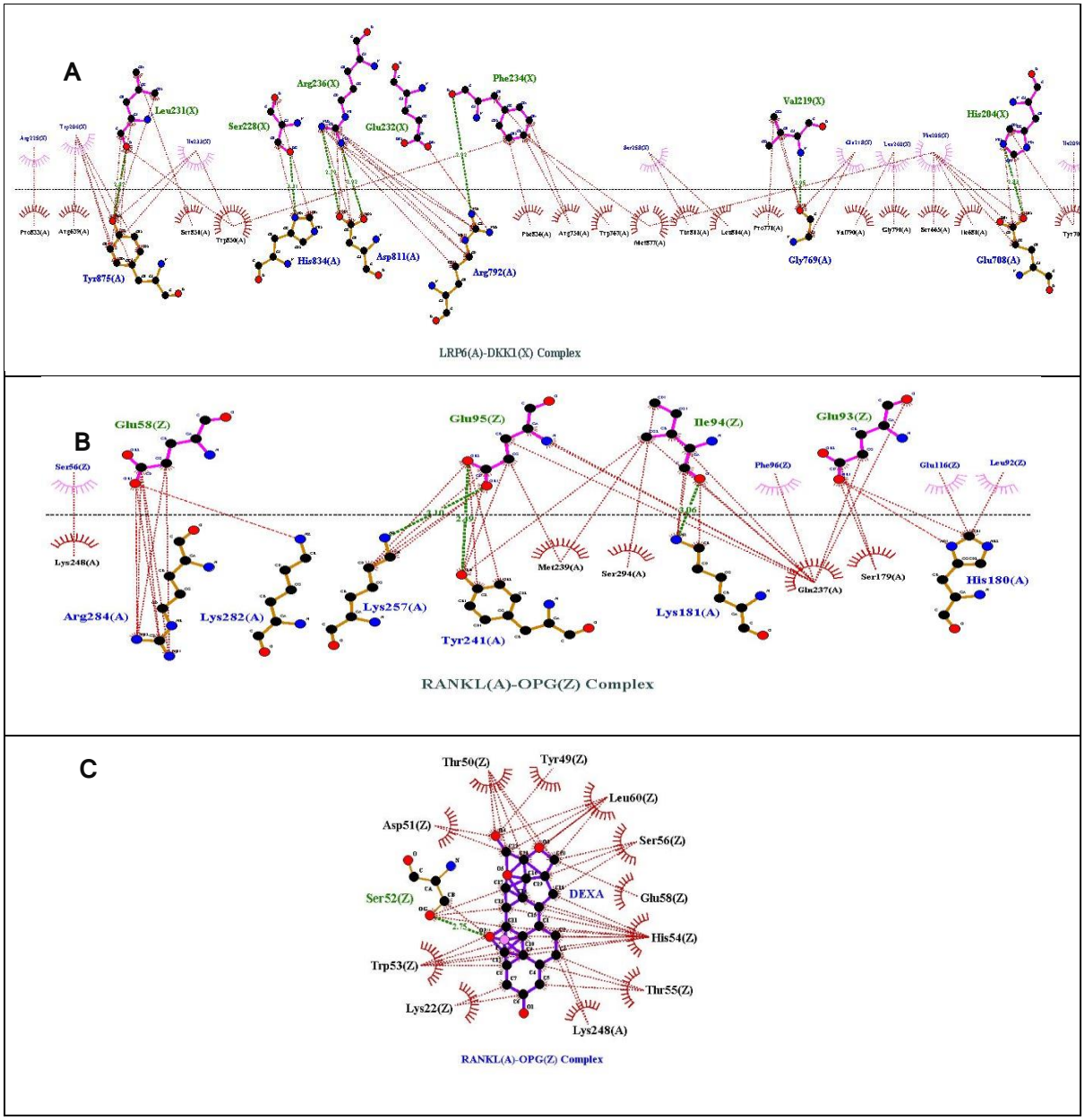

Fig. 2. 2D docked structures visualized by using LigPlot+ v.2.2.7 software. **A.** DEXA-LRP5/6 docked form. **B.** RANKL(A)-OPGB(Z) chains binding and interactions. **C.** DEXA-RANKL(A)-OPGB(Z) docked form. Dotted green lines represented the ligand-amino acid residue **(A)** and amino acid-amino acid residue **(B)** in H-bonds, and dotted red lines demonstrated the ligand-amino acid residue **(A)** and amino acid-amino acid residue **(B)** in hydrophobic interactions.

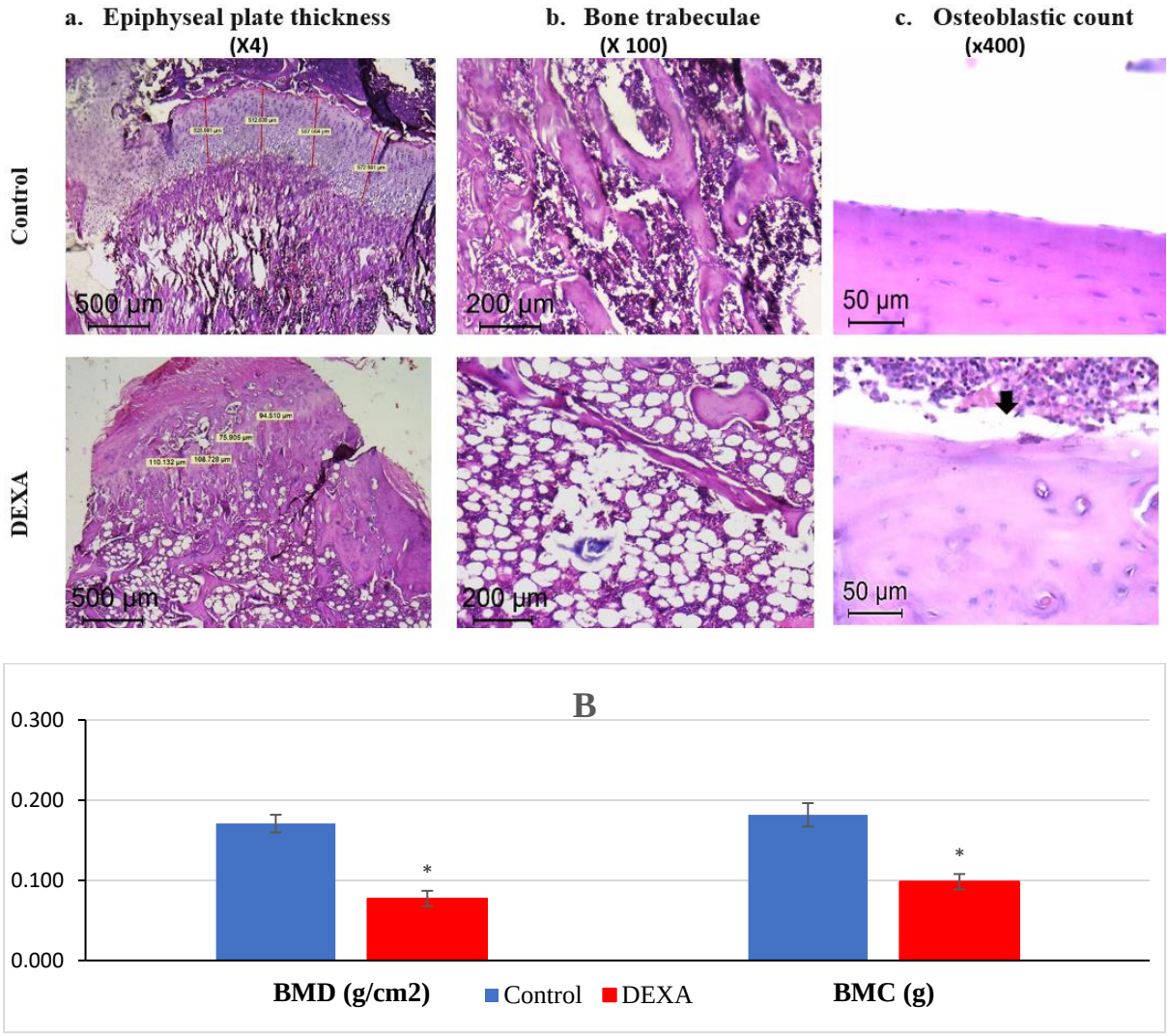

Fig. 3. (A) H&E-staining of rat femur. Control: (a) normal epiphyseal plate (×40), (b) normal architecture of bone trabeculae with normal bone marrow space. (c) high osteoblastic count on cortical bone surface (×400). DEXA: (a) narrowed epiphyseal plate (b) sporadic thinned bony ossicles disconnected by an extended bone marrow and amplified fat content (×100), (c) osteoblast rimming loss with enhanced osteoclastic activity with erosion cavity (arrow) (X400)**. (B)** Bone mineral density (BMD), and bone mineral content (BMC). Values are expressed as mean ± SD (n = 8 for BMD and BMC). *: significant ($p < 0.05$) compared to control.

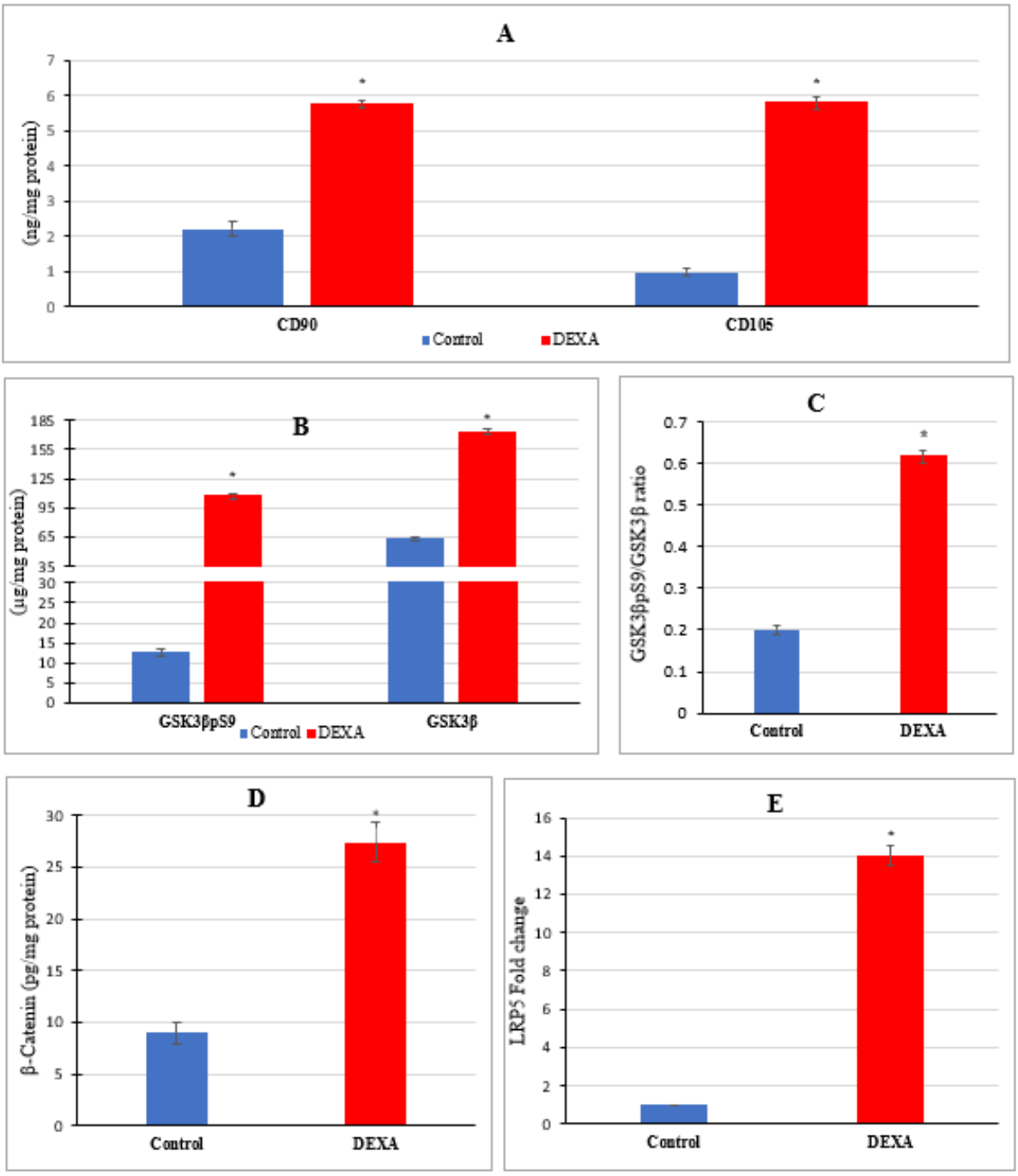

Fig. 4. Proliferation markers of the studied experimental groups. A) CD90 and CD105 bone protein contents. B) Bone protein content of each of GSK3βpS9 and GSK3β. C) Bone GSK3βpS9/GSK3β ratio. D) Bone protein content of β-catenin. E) Bone LRP5 fold change. D). Values are expressed mean ± SD (n = 8). *: significant ($P \leq 0.05$) compared to control.

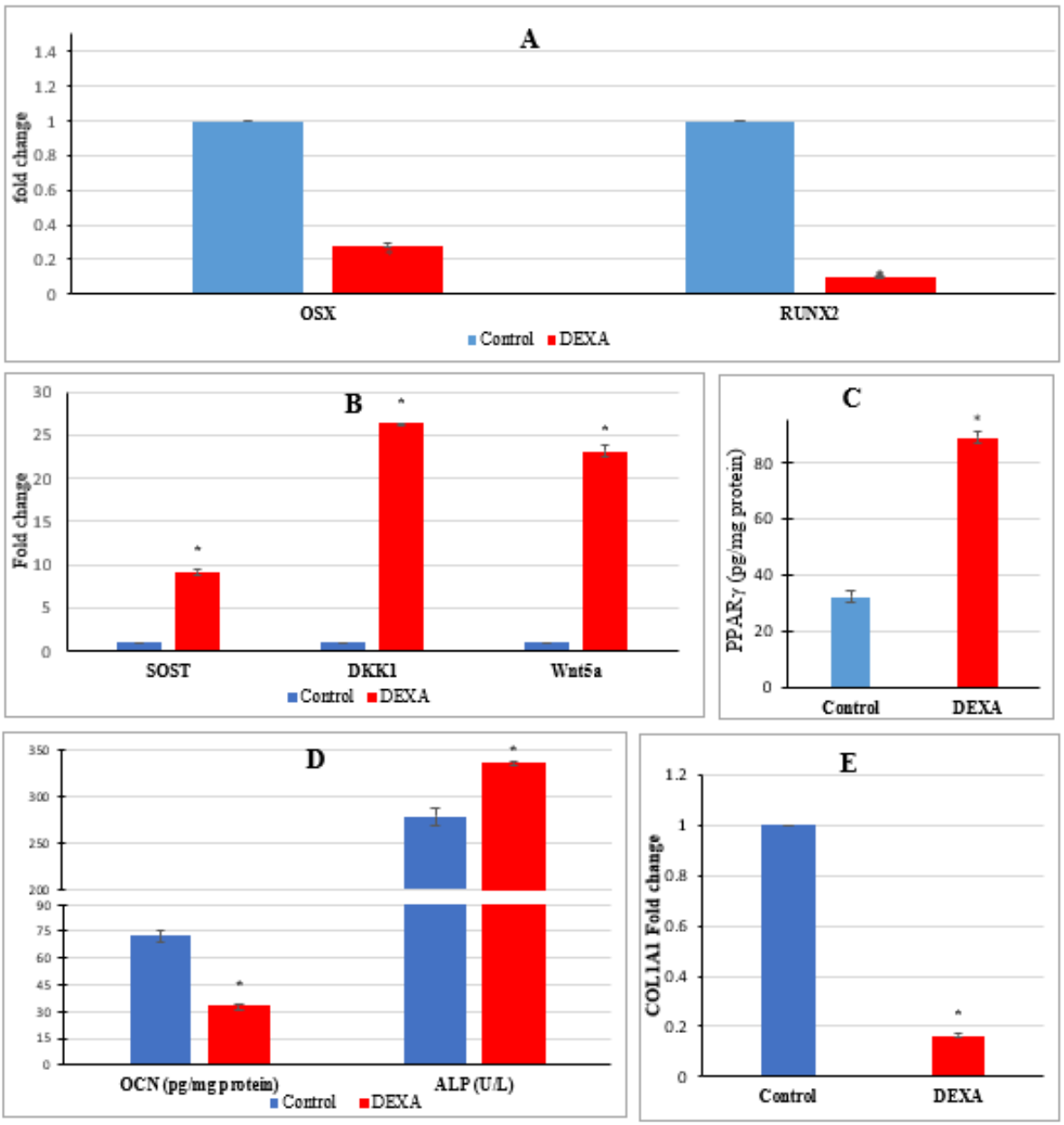

Fig .5. MSCs differentiation regulators and markers of different experimental groups. A) Bone RUNX2 and OSX expression. B) Bone SOST, DKK1 and WNT5a fold change. C) Bone protein content of each of PPARγ. D) Bone protein content of OCN and serum ALP activity. E) Bone CollA1 fold change. Values are expressed as mean ± SD (n = 8). *: significant ($P \leq 0.05$) compared to control.

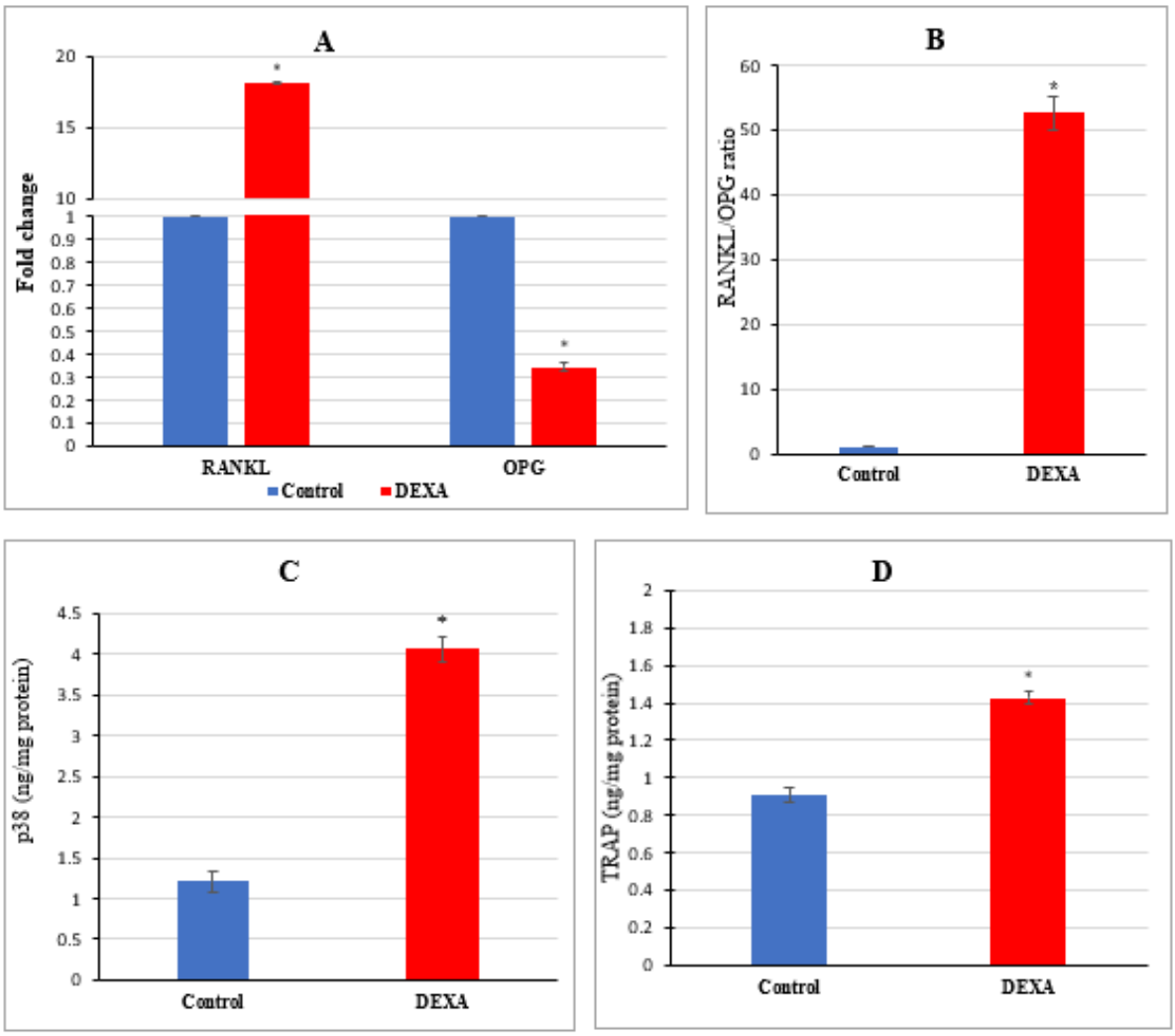

Fig. 6. HSCs markers of differentiation for the two experimental groups. A) Bone RANKL and OPG fold change. B) Bone RANKL/OPG ratio. C) Bone P38 protein content. D) Bone TRAP protein content. Values are expressed as mean ± SD (n = 8). *: significant ($P \leq 0.05$) compared to control.

7-Dexamethasone-Induced Femoral Oxidative Stress:

DEXA caused noticeable fluctuations in the oxidative stress indices in rat femurs as juxtaposed with rats receiving saline (Table 1). MDA and NO levels were significantly ($p < 0.05$) intensified. Whereas GSH content, in addition to the activities of SOD, GST, and GPx significantly ($p < 0.05$) declined compared to control rats.

Tab. 2. Bone pro- and anti- oxidant parameters.

	MDA level (µmol/ mg protein)	NO level (µmol/g protein)	GSH level (µmol/mg protein)	GPx activity (U/mg protein)	GST activity (U/mg protein)	SOD activity (U/mg protein)
Control	1.941±0.119	364.230± 16.678	10.198±0.520	53.228±5.810	0.785±0.061	1.226±0.077
DEXA	**2.400±0.052***	**862.260±16.930***	**6.397±0.250***	**22.792±1.578***	**0.403±0.026***	**0.995±0.062***
Values denote the mean ± SD of 8 rats/ group. *p ≤ 0.05 opposed to control applying ANOVA (one-way) and Post Hoc Test (Tukey's test).						

DISCUSSION

In this study, the standard imaging tests; BMD and BMC were used for the diagnosis of osteoporosis (Fahmy *et al.*, 2015). The declined BMD and BMC reported in rats receiving DEXA-approved previous findings (Samir and Malek, 2014; Chen *et al.*, 2016). These findings indicate incomplete bone mineralization represented by decreased bone formation, and increased bone resorption, suggesting the onset of osteoporosis (Cummings, 2007; Ahmed *et al.*, 2012; Samir and Malek, 2014).

GCs can inflict paradoxical actions upon bone tissue affecting the balanced bone remodeling. These actions are dependent on the stage of growth and differentiation of the cellular components, as well as the concentration and duration of GCs administration. Low GCs concentrations can motivate osteoblast proliferation and endorse MSCs/osteogenic differentiation. However, high GCs concentrations can induce osteoporosis by inhibiting osteoprogenitor cell proliferation and differentiation, stimulating apoptosis of osteoblast and osteocyte, decreasing their counts, and directing MSCs differentiation into adipocytes while inducing osteoclastogenesis (Delany, 1994; Mak *et al.*, 2009; Han *et al.*, 2019). CD90 (or Thy-1) and CD105 (or SH2) are cell surface markers that are crucial for cellular multipotency and immortality (Kim *et al.*, 2016). Proliferating MSCs have an intensified expression of CD90 and CD105. These cells can differentiate toward adipogenic and osteogenic lineages guided by the existing differentiation mediators and inhibitors (Maleki *et al.*, 2014; Ullah, Subbarao and Rho, 2015). A previous study reported that strong expression of CD105 might predict weak osteogenesis (Kim *et al.*, 2016). However, the expression of these CDs is not restricted to MSCs, in which HSCs are capable of expressing these markers (Wisniewski *et al.*, 2011; Kays *et al.*, 2015; Radtke *et al.*, 2020), where increased CD105 expression is correlated with long-term repopulating HSCs in mice (Kays *et al.*, 2015). Rats of the current study receiving DEXA displayed increased bone CD90 and CD105 protein contents. Based on the information provided previously, these elevations might be a sign of proliferating HSCs and/or MSCs induced by DEXA.

Wnt signaling is fundamental for the homeostasis, development, and regeneration of most body organs and is broadly conserved across cell types (Chae and Bothwell, 2018). GCs can alter the bone remodeling process by exerting a biphasic regulation of Wnt proteins and inhibitors (Mak *et al.*, 2009). Wnt signaling includes two main pathways: the β-catenin-dependent canonical Wnt pathway and the β-catenin-independent non-canonical Wnt pathway (Ackers and Malgor, 2018). GSK-3β is considered a negative director of the canonical Wnt signaling. While, activation of LRP5/Fzd receptor complex inhibits GSK3β through phosphorylation of GSK3β on serine9, stabilizing β-catenin for nuclear translocation and inducing gene activation (Doble and Woodgett, 2003; Kugimiya *et al.*, 2007). MSCs have an enrichment in the components of both canonical and non-canonical Wnt pathways, where the initiation of these pathways plays an indispensable task in the proliferation and differentiation of these cells (Takam Kamga *et al.*, 2021). Increased MSCs proliferation is associated with overexpression of LRP5 in a human MSC culture (Baksh, Genevieve M Boland and Tuan, 2007). Through altering Fzd receptor, LRP5 initiates the signal transduction of the canonical Wnt route increasing proliferation while inhibiting osteogenic differentiation (Baksh, Genevieve M. Boland and Tuan, 2007). Additionally, proliferating early osteoclast precursors demand initiation of the canonical Wnt/β-catenin pathway (Weivoda *et al.*, 2016). The current outcomes displayed an amplified GSK3βpS$_9$/GSK3β ratio in DEXA-treated rats, indicating an overriding deactivated form of GSK3β. Taken together with the increased bone β-catenin protein levels and LRP5 expression signify an overactivated

canonical Wnt/β-catenin pathway in DEXA-treated rats.

The dedication of human MSCs towards the osteoblastic lineage instead of the adipogenic lineage is achieved through preserving an active Wnt/β-catenin signal to secure the abundance of the critical β-catenin downstream goal necessary for maintaining the differentiated phenotype of mature osteoblasts; including the transcription factor RUNX2, and its downstream target OSX (Ahmadzadeh *et al.*, 2016). OSX is accountable for the expression of the osteoblast-related genes, COL1A1, OPG, and OCN (Marie, 1992; Bruderer *et al.*, 2014; Liu *et al.*, 2020). In the current study, a reduction in the osteogenic transcription factors (RUNX2 and OSX) correlated with their downstream targets; OCN, COL1A1, and OPG were reported following DEXA treatment, and are aligned with previous results (Samir and Malek, 2014; El-wakf, El-komy and Hassan, 2019; Wang *et al.*, 2020). These outcomes point toward a deactivated osteoblasts Wnt/β-catenin signal, hence we may relate the amplified canonical Wnt/β-catenin signal to proliferating MSC and osteoclast precursors, not the differentiating osteoblasts. The raised serum ALP activity following DEXA-treatment in this study, as well as previous studies (El-wakf, El-komy and Hassan, 2019; Saad, Mohamed and El-Gohary, 2019), may be due to the ability of DEXA to promote osteoblasts apoptosis, releasing its ALP in the environment and lastly increasing the serum ALP (Farley and Stilt-Coffing, 2001; Chotiyarnwong and McCloskey, 2020).

Wnt5a is "a non-canonical Wnt ligand" secreted by MSC, preadipocytes, and adipocytes (Guan *et al.*, 2014). It plays a part in controlling MSC proliferation and differentiation through inactivating PPARγ (a key adipogenic transcription factor), and activating $Runx_2$ (Etheridge *et al.*, 2004; Bilkovski *et al.*, 2010). Alternatively, DKK1 "Wnt inhibitor" secreted from MSC, can shift the differentiation of MSCs towards adipocytes through counteracting the inhibitory effect of Wnt5a over PPARγ. This will result in the activation of PPARγ and deactivation of RUNX2 stimulating adipogenesis (Etheridge *et al.*, 2004; Pinzone *et al.*, 2009; Bilkovski *et al.*, 2010).

In support of the ability of GCs to inhibit mesenchymal-osteoblast differentiation, Frenkel *et al* linked this inhibition partly through inhibiting the Wnt/β-catenin pathway, via overexpressing DKK1 and another Wnt pathway antagonist; SOST. Enhanced expression of these two genes has been reported in human osteoporotic MSCs (Frenkel *et al.*, 2015; Phetfong *et al.*, 2016). Furthermore, osteogenic differentiation inhibitors were found to be necessary to support proliferating MSCs (Pinzone *et al.*, 2009).

In this study, the increased bone PPARγ level in addition to the upregulated DKK1 and SOST, along with the decreased RUNX2 and OSX expression confirm the adipogenic fate of MSC in DEXA-treated rats instead of osteoblast differentiation. These findings are concomitant with previous reports (Frenkel *et al.*, 2015; Chen *et al.*, 2016; Phetfong *et al.*, 2016; Wang, Pan and Chen, 2019; Liu *et al.*, 2020). This explanation was further supported by the decreased number of osteoblasts and increased adiposity following DEXA administration detected in the microscopic assessment.

The current docking analysis was used to study the ability of DEXA to associate with several biological targets involved in Wnt /β-catenin signaling. The docking study revealed the existence of several associations between DEXA with LRP5/6 co-receptor, DKK1, and PPARγ. These associations represent a breakthrough in the ability of DEXA to directly interact and manipulate the functioning of these proteins in Wnt /β-catenin signal. However, we can't determine the exact effect of such interactions, because of the complexity and interference of other factors in Wnt /β-catenin signaling.

Even though a declined osteoblastic population was apparent in DEXA-treated rats of this study, an increased bone RANKL expression was also reported and is consistent

with previous outcomes (Chen *et al.*, 2016). This increased bone RANKL expression may be justified by the multi-origin of RANKL, where it can be expressed by a diversity of bone marrow cell types such as MSCs, osteoblast progenitors, and adipocytes (Robert Cronin Yung Peng, Rose Khavari, 2017; Kerensa *et al.*, 2019). Furthermore, activation of the canonical Wnt signal in osteoblast precursors is essential for downregulating RANKL expression and suppressing bone resorption (Maeda, Takahashi and Kobayashi, 2013). Hence the GC-induced repression of the Wnt/β-catenin in osteoblasts will result in an increased RANKL/OPG ratio favoring the RANKL-induced osteoclast differentiation. The increased ratio observed in the DEXA-treated rats is compatible with the findings of Tolba *et al.* (Tolba, El-Serafi and Omar, 2017). Moreover, it has been testified that Wnt5a signals osteoclast differentiation by encouraging RANK expression in osteoclasts (Kobayashi *et al.*, 2015; Ahmadzadeh *et al.*, 2016; Weivoda *et al.*, 2016). This increase indicates amplified bone resorption caused by the increased osteoclastogenesis and the consequent onset of osteoporosis. These outcomes are endorsed by the evident increased osteoclasts score in the histological results. Moreover, when RANKL binds to RANK, the downstream signaling p38-MAPK is activated, which ensures the abundant expression of osteoclast-linked genes such as TRAP (Matsumoto *et al.*, 2000; Kobayashi *et al.*, 2015; Thouverey and Caverzasio, 2015). Osteoclasts secrete acid phosphatases necessary to resolve the mineral part of bones. The isoenzyme of acid phosphatase; TRAP is involved in the resorption of bone and has been found to correlate directly with the activity of osteoclasts in bone (Bull *et al.*, 2002; Roux, 2006).

Consequently, the raised RANKL will ultimately increase the bone protein level of P38 as well as bone TRAP in rats of our study receiving DEXA. These findings agree with previous outcomes (Wang *et al.*, 2020), and confirm the increased osteoclastogenesis and bone resorption by DEXA (El-wakf, El-komy and Hassan, 2019). The present DEXA/RANKL/OPG docking study reveals the existence of associations between the components of this complex, and the presence of a direct effect of DEXA over the RANKL/OPG complex which might be partly in charge of the increased RANKL/RANK signaling through weakening the RANKL/OPG complex. Additionally, the present DEXA-TRAP docked form shows direct interactions between DEXA and TRAP. These interactions might be partly in charge of the increased activity of TRAP reported in this *in vivo* study.

Oxidative stress is a malicious factor implicated in the onset of osteoporosis (El Wakf, Hassan and Gharib, 2014). Reactive oxygen species (ROS) can raise membrane lipids peroxidation and increase MDA (El-wakf, El-komy and Hassan, 2019). Moreover, increased DKK1 expression was reported to be accompanied by oxidative stress (Colla *et al.*, 2007), suggesting that the increased expression of DKK1 in our study can be also related to oxidative stress.

GCs can directly expand oxidative stress by enhancing the production of ROS while overwhelming the activities of the antioxidant system (El-wakf, El-komy and Hassan, 2019). GCs can prompt osteoclastogenesis while extending the life span of osteoclasts, and this is achieved by decreasing the expression of SOD and GPx increasing intracellular ROS levels (Lee *et al.*, 2005; Kanzaki *et al.*, 2013; Tolba, El-Serafi and Omar, 2017). Previous findings reported decreased bone antioxidant components GSH, GST, GPx, GR, and catalase following GCs administration (Hozayen *et al.*, 2016), which is consistent with our outcomes. Furthermore, the findings of El-Wakf *et al.* are consistent with our reported raised oxidative stress marker MDA and diminished antioxidant components in the bone of DEXA-treated rats (El-Wakf, El-komy and Hassan, 2019). excess NO work against the proliferation of osteoblasts, while increasing their apoptosis. Furthermore, surplus NO can enhance osteoclast-mediated bone resorption

(Wimalawansa, 2010). Armour *et al*. reported in an inflammation-induced osteoporotic mice model, an increased NO production induced by the augmented activity of inducible nitric oxide synthase, which is compatible with our findings (Armour *et al.*, 2001).

Conclusion:

Glucocorticoids can impose osteoporosis by introducing alterations in canonical and non-canonical Wnt signaling and increasing oxidative stress in bone. These derangements disrupt the communication between bone remodeling components, resulting in a compelled proliferative phase on MSCs and HSCs. Consequently, proliferating MSCs increase the production of osteoclastogenic mediators, intensifying HSCs proliferation and unleashing their osteoclastic differentiation, increasing bone resorption, and decreasing bone formation causing bone fragility. Furthermore, inhibiting the canonical Wnt pathway in MSCs makes these cells deviate towards the adipogenic lineage.

Statements and Declarations:

1-Availability of Data And Materials:

The authors declare that the data supporting the findings of this study are available within the paper. Should any raw data files be needed in another format they are available from the corresponding author upon reasonable request. Source data are provided in this paper.

2-Ethics Approval:

All animal procedures obeyed the ARRIVE guidelines and were executed in compliance with the Institutional Animal Care and Use Committee (IACUC Protocol Approval No: 44-13M-9021), Alexandria University. This fulfills the guides for laboratory animal care and use announced by the National Institutes of Health (NIH Publications No. 8023). The study received an ethical clearance from the research ethics review committee, Alexandria University (04/23/04/27/634).

3-Competing Interests:

The authors have no relevant financial or non-financial interests to disclose.

4-Author Contributions:

All authors contributed to the study's conception and design. Adham M. Maher: Software, Data Curation, Writing, reviewing & editing original draft and final manuscript, Visualization; Samar R. Saleh: Methodology, Formal analysis, Investigation, Supervision, Validation, Software, Visualization, Data Curation, Writing, reviewing & editing original draft; Doaa A. Ghareeb: Conceptualization, Methodology, Resources, Supervision, Validation; Eman Sheta: Carried out and interpreted the histological examinations; Mohamed Nabil: Formal analysis, Investigation, Validation, Software; Fatema A. Younis: Carried out and interpreted the *in silico* study, Writing & editing the original draft, ; Aliaa A. Masoud: Formal analysis, Validation, Resources, Investigation, Software.

5-Funding Sources:

The authors declare that no funds, grants, or other support were received during the preparation of this manuscript.

Abbreviations:

ALP: Alkaline phosphatase, BSA: bovine serum albumin, CD: Cluster differentiation, COL1A1: Collagen type I alpha 1, COVID-19: Coronavirus disease 2019, DEXA: Dexamethasone, DKK1: Dickkopf-related protein 1, DTNB: 5,5'-dithio-bis-2-nitrobenzoic acid, EDTA: Ethylenediaminetetraacetic acid, ELISA: enzyme-linked immunosorbent assay, FoxO: Forkhead box O, Fzd: Frizzled, GAPDH: Glyceraldehyde 3-phosphate dehydrogenase, GCs: Glucocorticoids, GIO: Glucocorticoid-induced osteoporosis, GPx: Glutathione peroxidase, GR: Glutathione reductase, GSH: Reduced glutathione, GSK3β pS9: Glycogen synthase kinase 3 beta phosphorylated GSK3β at Serine9, GSK3β: Glycogen synthase kinase 3 beta, GST: Glutathione-S-transferase, H&E staining: Hematoxylin-eosin staining, HSCs: Hematopoietic stem cells, IACUC: Institutional Animal Care and Use Committee, LRP5: Low-density lipoprotein receptor-related protein-5, MDA: Malondialdehyde, MSCs: Mesenchymal stem cells, NO: nitric oxide, OCN: Osteocalcin,

OP: Osteoporosis, OPG: Osteoprotegerin, OSX: Osterix, (Liao *et al.*, 2017)p38-MAPKs: p38-Mitogen-activated protein kinases, PNPP: ρ-nitrophenyl phosphate, PPARγ: Peroxisome proliferator-activated receptor-γ, qRT-PCR: Quantitative real-time reverse transcription PCR analysis, RANKL: Receptor activator of nuclear factor kappa-B ligand, RNA: Ribonucleic acid, ROS: Reactive oxygen species, RUNX2: Runt-related transcription factor 2, SOD: Superoxide dismutase, SOST: Sclerostin, TBA: Trabecular bone area, TRAP: Tartrate resistance acid phosphatase, WNT5a: Wingless protein 5a.

REFERENCES

Ackers, I. and Malgor, R. (2018) 'Interrelationship of canonical and non-canonical Wnt signalling pathways in chronic metabolic diseases', *Diabetes and Vascular Disease Research*. SAGE Publications Ltd, pp. 3–13. doi: 10.1177/1479164117738442.

Ahmadzadeh, A. *et al.* (2016) 'Wnt/β-catenin signaling in bone marrow niche', *Cell and Tissue Research*, pp. 321–335. doi: 10.1007/s00441-015-2300-y.

Ahmed, H. H. *et al.* (2012) 'Potential role of leptin against glucocorticoid-induced secondary', *European review for medical and pharmacological sciences*, 16(10), pp. 1446–1452.

An, J. J. *et al.* (2007) 'Expression and regulation of osteoprotegerin in adipose tissue', *Yonsei Medical Journal*, 48(5), pp. 765–772. doi: 10.3349/ymj.2007.48.5.765.

Annane, D. (2021) 'Corticosteroids for COVID-19', *Journal of Intensive Medicine*, (November 2020), pp. 1–12. doi: 10.1016/j.jointm.2021.01.002.

Armour, K. J. *et al.* (2001) *Activation of the Inducible Nitric Oxide Synthase Pathway Contributes to Inflammation -Induced Osteoporosis by Suppressing Bone Formation and Causing Osteoblast Apoptosis*, *Arthritis & Rheumatism*.

Baksh, D., Boland, Genevieve M. and Tuan, R. S. (2007) 'Cross-talk between Wnt signaling pathways in human mesenchymal stem cells leads to functional antagonism during osteogenic differentiation', *Journal of Cellular Biochemistry*, 101(5), pp. 1109–1124. doi: 10.1002/JCB.21097.

Baksh, D., Boland, Genevieve M and Tuan, R. S. (2007) 'Cross-Talk Between Wnt Signaling Pathways in Human Mesenchymal Stem Cells Leads to Functional Antagonism During Osteogenic Differentiation', *Journal of Cellular Biochemistry*, 101, pp. 1109–1124. doi: 10.1002/jcb.21097.

Bancroft, J.D. and Gamble, M. and Burchette, J. (2009) *Theory and Practice of Histological Techniques*, *The American Journal of Dermatopathology*. doi: 10.1097/dad.0b013e31819e8d01.

Bilkovski, R. *et al.* (2010) 'Role of Wnt-5a in the determination of human mesenchymal stem cells into preadipocytes', *Journal of Biological Chemistry*, 285(9), pp. 6170–6178. doi: 10.1074/jbc. M109.054338.

Bitto, A. *et al.* (2009) 'Protective effect of genistein aglycone on the development of osteonecrosis of the femoral head and secondary osteoporosis induced by methylprednisolone in rats', *Journal of Endocrinology*, 201(3), pp. 321–328. doi: 10.1677/JOE-08-0552.

Bruderer, M. *et al.* (2014) 'Role and regulation of runx2 in osteogenesis', *European Cells and Materials*, 28, pp. 269–286. doi: 10.22203/eCM.v028a19.

Buckingham, J. C. (2006) 'Glucocorticoids: Exemplars of multi-tasking', *British Journal of Pharmacology*, 147(SUPPL. 1), pp. 258–268. doi: 10.1038/sj.bjp.0706456.

Bull, H. *et al.* (2002) 'Acid phosphatases', *Journal of Clinical Pathology - Molecular Pathology*. BMJ Publishing Group Ltd, pp. 65–72. doi: 10.1136/mp.55.2.65.

Caricasole, A. *et al.* (2004) 'Induction of Dickkopf-1, a negative modulator of the Wnt pathway, is associated with neuronal degeneration in Alzheimer's brain', *Journal of Neuroscience*, 24(26), pp. 6021–6027. doi: 10.1523/JNEUROSCI. 1381-04.2004.

Chae, W. J. and Bothwell, A. L. M. (2018) 'Canonical and Non-Canonical Wnt Signaling in Immune Cells', *Trends in Immunology*, 39(10), pp. 830–847. doi: 10.1016/j.it.2018.08.006.

Chalmers, G. L. (1978) 'Disorders of bone', *Practitioner*, 220(1319), pp. 711–721. doi: 10.3109/9780203508954-27.

Chen, Z. *et al.* (2016) 'Curcumin alleviates glucocorticoid-induced osteoporosis through the regulation of the Wnt signaling pathway', *International Journal of Molecular Medicine*, 37(2), pp. 329–338. doi: 10.3892/ijmm.2015.2432.

Cheng, Z. *et al.* (2011) 'Crystal structures of the extracellular domain of LRP6 and its complex with DKK1.', *Nature structural & molecular biology*, 18(11), pp. 1204–1210. doi: 10.1038/nsmb.2139.

Chiodini, I. *et al.* (2020) 'Treatment options for glucocorticoid-induced osteoporosis', *Expert Opinion on Pharmacotherapy*, 21(6), pp. 721–732. doi: 10.1080/14656566.2020.1721467.

Chotiyarnwong, P. and McCloskey, E. V. (2020) 'Pathogenesis of glucocorticoid-induced osteoporosis and options for treatment', *Nature Reviews Endocrinology*, 16(8), pp. 437–447. doi: 10.1038/s41574-020-0341-0.

Colla, S. *et al.* (2007) 'The oxidative stress response regulates DKK1 expression through the JNK signaling cascade in multiple myeloma plasma cells', *Blood*, 109(10), pp. 4470–4477. doi: 10.1182/blood-2006-11-056747.

Cronet, P. *et al.* (2001) 'Structure of the PPARα and -γ ligand binding domain in complex with AZ 242; ligand selectivity and agonist activation in the PPAR family', *Structure*, 9(8), pp. 699–706. doi: 10.1016/S0969-2126(01)00634-7.

Cummings, S. R. (2007) 'CLINICIAN ' S CORNER Clinical Use of Bone Densitometry Scientific Review', *October*, 288(15), pp. 1889–1897.

Delany, A. M., Dong, Y. and Canalis, E. (1994) 'Mechanisms of glucocorticoid action in bone cells', *Journal of Cellular Biochemistry*, 56(3), pp. 295–302. doi: 10.1002/jcb.240560304.

Doble, B. W. and Woodgett, J. R. (2003) *GSK-3: Tricks of the trade for a multi-tasking kinase, Journal of Cell Science*. doi: 10.1242/jcs.00384.

El-wakf, A. M., El-komy, M. A. and Hassan, D. G. (2019) 'Preventive effect of dried plum extract against dexamethasone-induced osteoporosis in male rats through inhibiting cathepsin-K activity , lipogenesis and trabecular bone loss', *Journal of Innovations in Pharmaceutical and Biological Sciences (JIPBS)*, Vol 6 (2)(2), pp. 52–61.

Ellman, G. L. (1959) 'Tissue sulfhydryl groups', *Archives of Biochemistry and Biophysics*, 82(1), pp. 70–77. doi:10.1016/0003-9861(59)90090-6

Etheridge, S. L. *et al.* (2004) 'Expression Profiling and Functional Analysis of Wnt Signaling Mechanisms in Mesenchymal Stem Cells', *Stem Cells*, 22(5), pp. 849–860. doi: 10.1634/stemcells.22-5-849.

Fahmy, S. R. *et al.* (2015) 'Possible antiosteoporotic mechanism of cicer arietinum extract in ovariectomized rats', *International Journal of*

Clinical and Experimental Pathology, 8(4), pp. 3477–3490.

Farley JR, Stilt-Coffing B. Apoptosis may determine the release of skeletal alkaline phosphatase activity from human osteoblast-line cells. Calcif Tissue Int. 2001 Jan;68(1):43-52. doi: 10.1007/BF02685002. Epub 2001 Feb 23. PMID: 12037623.

Frenkel, B. *et al.* (2015) Glucocorticoid-Induced osteoporosis, *Advances in Experimental Medicine and Biology*. doi: 10.1007/978-1-4939-2895-8_8.

Gaillard, T. (2018) 'Evaluation of AutoDock and AutoDock Vina on the CASF-2013 Benchmark.', *Journal of chemical information and modeling*, 58(8), pp. 1697–1706. doi: 10.1021/acs.jcim.8b00312.

García-Moreno, P. J. *et al.* (2023) 'Recent advances in the production of emulsifying peptides with the aid of proteomics and bioinformatics', *Current Opinion in Food Science*, 51, p. 101039. doi: https://doi.org/10.1016/j.cofs.2023.101039.

Guan, S. *et al.* (2014) 'Wnt5a is associated with the differentiation of bone marrow mesenchymal stem cells in vascular calcification by connecting with different receptors', *Molecular Medicine Reports*, 10(4), pp. 1985–1991. doi: 10.3892/mmr.2014.2449.

Habig, W. H., Pabst, M. J. and Jakoby, W. B. (1974) 'Glutathione S transferases. The first enzymatic step in mercapturic acid formation', *Journal of Biological Chemistry*, 249(22), pp. 7130–7139. doi: 10.1016/S0021-9258(19)42083-8.

Han, J. *et al.* (2015) 'Expression of ATF4 and RUNX2 in periodontal tissue of pressure side during orthodontic tooth movement in rat', *International Journal of Clinical and Experimental Medicine*, 8(1), pp. 934–938.

Han, L. *et al.* (2019) 'The shift in the balance between osteoblastogenesis and adipogenesis of mesenchymal stem cells mediated by glucocorticoid receptor', *Stem Cell Research and Therapy*, 10(1), pp. 1–14. doi: 10.1186/s13287-019-1498-0.

Hozayen, W. G. *et al.* (2016) 'Antiosteoporotic effect of Petroselinum crispum, Ocimum basilicum and Cichorium intybus L. in glucocorticoid-induced osteoporosis in rats', *BMC Complementary and Alternative Medicine*, 16(1), pp. 1–11. doi: 10.1186/s12906-016-1140-y.

Jung, L. *et al.* (2008) 'Glucocorticoids in the treatment of joint surgery', *Central-European Journal of Immunology*, 33(3), pp. 153–157.

Kanzaki, H. *et al.* (2013) 'The Keap1/Nrf2 protein axis plays a role in osteoclast differentiation by regulating intracellular reactive oxygen species signaling', *Journal of Biological Chemistry*, 288(32), pp. 23009–23020. doi: 10.1074/jbc.M113.478545.

Kays, S. K. *et al.* (2015) 'CD105 is a surface marker for receptor-targeted gene transfer into human long-term repopulating hematopoietic stem cells', *Stem Cells and Development*, 24(6), pp. 714–723. doi: 10.1089/scd.2014.0455.

Kerensa, X. *et al.* (2019) 'Ovariectomy increases RANKL protein expression in bone marrow adipocytes of C3H/HeJ mice', *American Journal of Physiology-Endocrinology and Metabolism*, 317, pp. 1050–1054. doi: 10.1152/ajpendo.00142.2019.-Estrogen.

Kim, Y.-K. *et al.* (2016) 'Osteogenic Potential of Mouse Periosteum-Derived Cells Sorted for CD90 In Vitro and In Vivo', *STEM CELLS Translational Medicine*, 5(2), pp. 227–234. doi: 10.5966/sctm.2015-0013.

Kobayashi, Y. *et al.* (2015) 'The regulation of osteoclast differentiation by Wnt signals', *BoneKEy Reports*, 4, p.

713. doi: 10.1038/bonekey.2015.82.

Kugimiya, F. *et al.* (2007) 'GSK-3β controls osteogenesis through regulating Runx2 activity', *PLoS ONE*, 2(9). doi: 10.1371/journal.pone.0000837.

Lee, N. K. *et al.* (2005) 'A crucial role for reactive oxygen species in RANKL-induced osteoclast differentiation', *Blood*, 106(3), pp. 852–859. doi: 10.1182/blood-2004-09-3662.

Liao, X. *et al.* (2017) 'The sirt6 gene: Does it play a role in tooth development?', *PLoS ONE*, 12(3), pp. 0174255–0174255. doi: 10.1371/journal.pone.0174255.

Lin, J. T. and Lane, J. M. (2004) 'Osteoporosis: A review', *Clinical Orthopaedics and Related Research*, (425), pp. 126–134. doi: 10.1097/01.blo.0000132404.30139.f2.

Liu, Q. *et al.* (2020) 'Recent Advances of Osterix Transcription Factor in Osteoblast Differentiation and Bone Formation', *Frontiers in Cell and Developmental Biology*, 8 (December). doi: 10.3389/fcell.2020.601224.

Low, J. L. *et al.* (2021) 'Molecular docking-aided identification of small molecule inhibitors targeting β-catenin-TCF4 interaction', *iScience*, 24(6). doi: 10.1016/j.isci.2021.102544.

Lu, S. Y. *et al.* (2017) 'The osteogenesis-promoting effects of alpha-lipoic acid against glucocorticoid-induced osteoporosis through the NOX4, NF-kappaB, JNK and PI3K/AKT pathways', *Scientific Reports*, 7(1), pp. 3331–3331. doi: 10.1038/s41598-017-03187-w.

Luan, X. *et al.* (2012) 'Crystal structure of human RANKL complexed with its decoy receptor osteoprotegerin.', *Journal of immunology (Baltimore, Md. : 1950)*, 189(1), pp. 245–252. doi: 10.4049/jimmunol.1103387.

Maeda, K., Takahashi, N. and Kobayashi, Y. (2013) 'Roles of Wnt signals in bone resorption during physiological and pathological states', *Journal of Molecular Medicine*, 91(1), pp. 15–23. doi: 10.1007/s00109-012-0974-0

Maher, A. M. *et al.* (2020) 'Exogenous melatonin restrains neuroinflammation in high fat diet induced diabetic rats through attenuating indoleamine 2,3-dioxygenase 1 expression', *Life Sciences*, 247, p. 117427. doi: 10.1016/j.lfs.2020.117427.

Mak, W. *et al.* (2009) 'Biphasic Glucocorticoid-dependent regulation of Wnt expression and its inhibitors in mature osteoblastic cells', *Calcified Tissue International* ,85(6), pp. 538–545. doi: 10.1007/s00223-009-9303-1.

Maleki, M. *et al.* (2014) 'Comparison of mesenchymal stem cell markers in multiple human adult stem cells', *International Journal of Stem Cells*, 7(2), pp. 118–126. doi: 10.15283/ijsc.2014.7.2.118.

Marie, P. (1992) 'Physiology of bone tissue', *Immuno-analyse & Biologie Spécialisée*, 7(6), pp. 17–24. doi: 10.1016/S0923-2532(05)80182-6.

Marklund, S. and Marklund, G. (1974) 'Involvement of the Superoxide Anion Radical in the Autoxidation of Pyrogallol and a Convenient Assay for Superoxide Dismutase', *European Journal of Biochemistry*, 47(3), pp. 469–474. doi: 10.1111/j.1432-1033.1974.tb03714.x.

Martin, T. J., Sims, N. A. and Quinn, J. M. W. (2011) *Interactions Among Osteoblasts, Osteoclasts, and Other Cells in Bone*, *Osteoimmunology* .Academic press, doi: 10.1016/b978-0-12-375670-1.10008-1.

Matsumoto, M. *et al.* (2000) 'Involvement of p38 mitogen-activated protein kinase signaling pathway in osteoclastogenesis mediated by receptor activator of NF-κB ligand (RANKL)', *Journal of Biological Chemistry*, 275(40), pp. 31155–31161. doi: 10.1074/jbc.M00

1229200.

Montgomery, H.A.C. and Dymock, J. (1961) *The determination of nitrite in water.*, *Scientific Research Publishing*. Available at: https://www.scirp.org/(S(oyulxb452alnt1aej1nfow45))/reference/ReferencesPapers.aspx?ReferenceID=882955 (Accessed: 19 May 2021).

Nalli, M. *et al.* (2022) 'Emerging Direct Targeting β-Catenin Agents', *Molecules*, 27(22), pp. 1–15. doi: 10.3390/molecules27227735.

Paglia, D. E. and Valentine, W. N. (1967) 'Studies on the quantitative and qualitative characterization of erythrocyte glutathione peroxidase', *The Journal of Laboratory and Clinical Medicine*, 70(1), pp. 158–169. doi: 10.5555/uri:pii:0022214367900765.

Phetfong, J. *et al.* (2016) 'Osteoporosis: the current status of mesenchymal stem cell-based therapy', *Cellular & molecular biology letters*, 21(1), pp. 12–12. doi: 10.1186/s11658-016-0013-1.

Pinzone, J. J. *et al.* (2009) 'The role of Dickkopf-1 in bone development, homeostasis, and disease', *Blood*, 113(3), pp. 517–525. doi: 10.1182/blood-2008-03-145169.

Pizzino, G. *et al.* (2017) 'Adenosine receptor stimulation improves glucocorticoid -induced osteoporosis in a rat model', *Frontiers in Pharmacology*, 8(SEP), pp. 558–558. doi: 10.3389/fphar.2017.00558.

Radtke, S. *et al.* (2020) 'Purification of Human CD34+CD90+ HSCs Reduces Target Cell Population and Improves Lentiviral Transduction for Gene Therapy', *Molecular Therapy - Methods and Clinical Development*, 18(September), pp. 679–691. doi: 10.1016/j.omtm.2020.07.010.

Rhen, T. and Cidlowski, J. A. (2005) 'Antiinflammatory Action of Glucocorticoids — New Mechanisms for Old Drugs', *New England Journal of Medicine*, 353(16), pp. 1711–1723. doi: 10.1056/nejmra050541.

Robert Cronin Yung Peng, Rose Khavari, N. D. (2017) 'Matrix-embedded cells control osteoclast formation', *Physiology & behavior*, 176(3), pp. 139–148. doi: 10.1038/nm. 2448. Matrix-embedded.

Roux, C. (2006) 'Biochemical markers of bone remodeling', *Revue Francophone des Laboratoires*, 2006(379 SUPPL. 1), pp. 32–33. doi: 10.1016/S1773-035X(06)80048-1.

Saad, D., Mohamed, A. E.-H. and El-Gohary, S. (2019) 'Green tea extract suppresses osteoclastogenesis and opposes glucocorticoid-induced osteoporosis in rats', *Journal of The Arab Society for Medical Research*, 14(1), p. 33. doi: 10.4103/jasmr.jasmr_10_19.

Samir, S. M. and Malek, H. A. (2014) 'Effect of cannabinoid receptors 1 modulation on osteoporosis in a rat model of different ages', *Journal of Physiology and Pharmacology*, 65(5), pp. 687–694.

Saud, B., Malla, R. and Shrestha, K. (2019) 'A Review on the Effect of Plant Extract on Mesenchymal Stem Cell Proliferation and Differentiation'. doi: 10.1155/2019/7513404.

Sträter, N. *et al.* (2005) 'Crystal structures of recombinant human purple Acid phosphatase with and without an inhibitory conformation of the repression loop.', *Journal of molecular biology*, 351(1), pp. 233–246. doi: 10.1016/j.jmb.2005.04.014.

Sui, X. *et al.* (2018) 'Cellular Physiology and Biochemistry Cellular Physiology and Biochemistry Constitutive Activation of β-Catenin in Differentiated Osteoclasts Induces Bone Loss in Mice', *Cell Physiol Biochem*, 48, pp. 2091–2102. doi:

10.1159/000492549.

Takahashi, M. *et al.* (2010) 'Dosing-time dependent effect of dexamethasone on bone density in rats', *Life Sciences*, 86(1–2), pp. 24–29. doi: 10.1016/j.lfs.2009.10.020.

Takam Kamga, P. *et al.* (2021) 'The Role of Notch and Wnt Signaling in MSC Communication in Normal and Leukemic Bone Marrow Niche', *Frontiers in Cell and Developmental Biology*, 8(January). doi: 10.3389/fcell.2020.599276.

Tappel, A. L. and Zalkin, H. (1960) 'Inhibition of Lipid Peroxidation in Microsomes by Vitamin e', *Nature*, 185(4705), p. 35. doi: 10.1038/185035a0.

Thouverey, C. and Caverzasio, J. (2015) 'Focus on the p38 MAPK signaling pathway in bone development and maintenance', *BoneKEy Reports*, 4(JUNE), pp. 1–8. doi: 10.1038/bonekey.2015.80.

Tolba, M. F., El-Serafi, A. T. and Omar, H. A. (2017) 'Caffeic acid phenethyl ester protects against glucocorticoid-induced osteoporosis in vivo: Impact on oxidative stress and RANKL/OPG signals', *Toxicology and Applied Pharmacology*, 324, pp. 26–35. doi: 10.1016/j.taap. 2017. 03.021.

Ullah, I., Subbarao, R. B. and Rho, G. J. (2015) 'Human mesenchymal stem cells - Current trends and future prospective', *Bioscience Reports*, 35. doi: 10.1042/BSR20150025.

Vandewalle, J. *et al.* (2018) 'Therapeutic Mechanisms of Glucocorticoids', *Trends in Endocrinology and Metabolism*, 29(1), pp. 42–54. doi: 10.1016/j.tem.2017.10.010.

El Wakf, A. M., Hassan, H. A. and Gharib, N. S. (2014) 'Osteoprotective effect of soybean and sesame oils in ovariectomized rats via estrogen-like mechanism', *Cytotechnology*, 66(2), pp. 335–343. doi: 10.1007/s10616-013-9580-4.

Wang, Y. *et al.* (2020) 'Daphnetin ameliorates glucocorticoid-induced osteoporosis via activation of Wnt/GSK-3β/β-catenin signaling', *Toxicology and Applied Pharmacology*, 409(October), p. 115333. doi: 10.1016/j.taap. 2020. 115333.

Wang, Y., Pan, Z. and Chen, F. (2019) 'Inhibition of PPARc by bisphenol A diglycidyl ether ameliorates dexamethasone- induced osteoporosis in a mouse model', *Journal of International Medical Research*, 47(12), pp. 6268–6277. doi: 10.1177/0300060519870723.

Wang, Z., Li, Z. and Ji, H. (2021) 'Direct Targeting of β-Catenin in the Wnt Signaling Pathway: Current Progress and Perspectives', *Medicinal research reviews*, 41(4), p. 2109. doi: 10.1002/MED.21787.

Weivoda, M. M. *et al.* (2016) 'Wnt Signaling Inhibits Osteoclast Differentiation by Activating Canonical and Noncanonical cAMP/PKA Pathways', *Journal of Bone and Mineral Research*, 31(1), pp. 65–75. doi: 10.1002/jbmr.2599.

Wimalawansa, S. J. (2010) 'Nitric oxide and bone', *Annals of the New York Academy of Sciences*, 1192(May), pp. 391–403. doi: 10.1111/j.1749-6632.2009.05230.x.

Wisniewski, D. *et al.* (2011) 'Further phenotypic characterization of the primitive lineage- CD34+CD38-CD90+CD45RA- Hematopoietic stem cell/progenitor cell sub-population isolated from cord blood, mobilized peripheral blood and patients with chronic myelogenous leukemia', *Blood Cancer Journal*, 1(9), pp. e36-11. doi: 10.1038/bcj.2011.35.

ARABIC SUMMARY

الآثار المترتبة على تغيير إشارات DKK1 / LRP / β-catenin في اضطراب إعادة تشكيل العظام الناجم عن الديكساميثازون: دراسات السيليكو وفي الجسم الحي لذكور الجرذان

أدهم ماهر[1]*, سمر صالح[1], دعاء غريب[1], إيمان شتا[2], محمد نبيل[3], فاطمة يونس[1], علياء مسعود[1]
[1]قسم الكيمياء الحيوية، كلية العلوم، جامعة الإسكندرية، الإسكندرية، 21511، مصر.
[2]قسم الباثولوجيا، كلية الطب، جامعة الإسكندرية. [3]قسم علم الأدوية، كلية الصيدلة، جامعة الوادي الجديد، الخارجة 72511، مصر

يمثل تناول الجلوكورتيكويدات على المدى الطويل المصدر الرئيسي لهشاشة العظام الثانوي، مما يعرض العظام لخطر للكسر والتاكل. تقدم الدراسة الحالية منظورا جديدا فيما يتعلق بتغيرات في إشارات Wnt/β-catenin الخاصة بهشاشة العظام المستحث بالديكساميثازون وذلك من خلال دراسة بعض العلامات المشاركة في تكاثر وتمايز خلايا إعادة تشكيل العظام الرئيسية و ذلك عبرالاستعانة بدراسات المحاكاة بالحاسوب وفي الجسم الحي. لتحليل المعلوماتية الحيوية، تم استخدام نماذج سيليكو لتصور وتقييم ارتباط الديكساميثازون تجاه معاملات إعادة تشكيل العظام الرئيسية. فيما يتعلق بالدراسة التي أجريت في الجسم الحي، تم تقسيم ستة عشر من ذكور جرذان السبراغ داولي البالغين إلى: مجموعة ضابطة تم إعطاؤها محلول ملحي، وتم إستحثاث مجموعة الاصابة بهشاشة العظام عن طريق حقن 1 ملجم / كجم من وزن الجسم بالديكساميثازون داخل الصفاق يوميًا لمدة 6 أسابيع. و قد أظهرت الدراسة السيليكو الارتباط والتفاعلات بين الديكساميثازون ومعاملات إعادة تشكيل العظام الرئيسية. كما تسبب الديكساميثازون في استحثاث هشاشة العظام وذلك كان واضحا من خلال كلا من الفحص المجهري لعظم الفخذ، وزيادة الإجهاد التأكسدي في عظم الفخذ، وارتفاع علامات التوالد، وارتفاع مثبط تمايز الخلايا البانية للعظم، وتناقص علامات تمايز الخلايا البانية للعظم ، وزيادة علامات التمايز لكلا من الخلايا ناقضة للعظم والخلايا الشحمية. مما سبق يتضح ان هشاشة العظام الناجمة عن الجلوكورتيكويدات تنشئ من خلال التوالد المكثف للخلايا الجذعية المكونة للدم والخلايا الجذعية الميزنكيمية عبر تصعيد وتغيير إشارات Wnt، التي تعمل بمثابة وسيلة تواصل بين مجموعتي الخلايا. أدت هذه التعديلات إلى تغيير مسار تمايز الخلايا الجذعية الميزنكيمية من مسار الخلايا البانية للعظم إلى المسار الشحمي وتسريع تمايز الخلايا ناقضة للعظم.